FULL PAPER

Dalton
www.rsc.org/dalton

Tris(pentafluorophenyl)borane adducts of substituted imidazoles: conformational features and chemical behavior upon deprotonation

Dominik Vagedes, Gerhard Erker,* Gerald Kehr,† Klaus Bergander,† Olga Kataeva,‡ Roland Fröhlich,‡ Stefan Grimme§ and Christian Mück-Lichtenfeld§

Organisch-Chemisches Institut der Universität Münster, Corrensstrasse 40, D-48149 Münster, Germany. E-mail: erker@uni-muenster.de; Fax: +49 (251) 83 36503

Received 15th October 2002, Accepted 5th February 2003
First published as an Advance Article on the web 3rd March 2003

Tris(pentafluorophenyl)borane adds to the donor nitrogen atom of 1,4,5-trimethyl- and 1-methyl-4,5-diphenylimidazole (**5a**,**b**) to yield the corresponding adducts **6a** and **6b**, respectively. Treatment of 1-methylbenzimidazole with $B(C_6F_5)_3$ or $B(C_6H_5)_3$ gave the related adducts **6c** and **7**, respectively. All four adducts were characterized by X-ray diffraction. In solution, the compounds **6** exhibit dynamic ^{19}F NMR spectra, each featuring 15 separate ^{19}F NMR resonances at low temperature. With increasing temperature a coalescence of the *o*-, *m*- and *p*-F signals of only a pair of $-C_6F_5$ signals is observed, leaving the set of five resonances of the third $-C_6F_5$ group unchanged. It required a further increase of the monitoring temperature to eventually observe the coalescence of the respective signals of all three $-C_6F_5$ groups. A DFT study revealed no specific intramolecular interactions of the F–C(Ar) substituents with other moieties of the molecules **6**; a topological control is thus likely to have caused this remarkably specific dynamic behavior. Deprotonation of the compounds **6a** and **6c** at carbon atom C2 was achieved by treatment with methyllithium. The expected "Arduengo carbene anions" (**8**) are, however, not stable under the reaction conditions but rapidly react by an intramolecular nucleophilic aromatic substitution at one of the adjacent $-C_6F_5$ groups to yield the heterotricyclic products **9**. The respective benzimidazole-derived compound **9c** was also characterized by an X-ray crystal structure analysis.

Introduction

The chemistry of N,N′-disubstituted imidazol-2-ylidenes (**1**) (Scheme 1) ("Arduengo carbenes")[1] has found much interest in recent years. These systems represent rare examples of stable and isolable carbene systems,[2] and they have found some application as ligands in transition metal catalysis.[3] Substitution of one of the groups attached to nitrogen by a borane would result in the generation of the anionic analogues of the neutral imidazol-2-ylidenes. Such "Arduengo carbene anions" could be envisaged *e.g.* as novel, very useful ligand systems in organotransition metal chemistry.

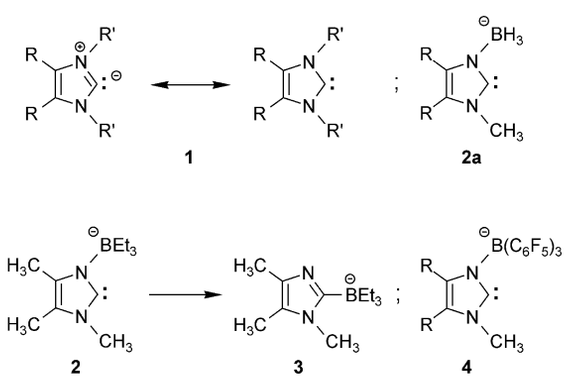

Scheme 1

To the best of our knowledge, only a single simple example of such a system has been published as yet. Siebert and coworkers have prepared and described the corresponding BH_3 adduct (**2a**).[4] Attempts to synthesize the corresponding BR_3 (R = aryl or alkyl) systems has invariably resulted in the formation of their C-bonded isomers (**3**). In a combined experimental and theoretical study we have recently shown that the corresponding anionic carbene systems **2** are unstable with regard to rearrangement to their thermodynamically favored isomers **3** which takes place by an intermolecular reaction pathway.[5] However, the respective imidazol-2-ylidenes could be shown to be generated as reactive intermediates in the case of the $B(C_6F_5)_3$ adducts (**4**) because here intramolecular S_{NAr}-fluoride displacement is more rapid than the otherwise ubiquitous intermolecular borane transfer.

We have now prepared a small series of substituted imidazole tris(pentafluorophenyl)borane adducts and found that they display an unconventional dynamic conformational behavior. Deprotonation of these systems probably generates the "anionic Arduengo carbenes" as reactive intermediates that react by subsequent ring-closure due to a rapid intramolecular nucleophilic aromatic substitution. An example of the resulting tricyclic intramolecular borane–imidazole adducts was, for the first time, characterized by X-ray diffraction, which is also described in this paper.

Results and discussion

Synthesis and structural characterization

For this study we have prepared the $B(C_6F_5)_3$ adducts[6,7] of 1,4,5-trimethylimidazole (**5a**), 1-methyl-4,5-diphenylimidazole (**5b**) and 1-methylbenzimidazole (**5c**). For the purpose of structural comparison, we have also prepared the BPh_3 adduct of **5c**, that was obtained crystalline for an X-ray crystal structure analysis. The reactions of the reagents **5** with tris(pentafluorophenyl)borane were carried out in pentane at room temperature (Scheme 2). The clean adducts precipitated from the reaction mixtures as white solids during a period of *ca.* 12 h, after which time the adduct formation was practically complete.

The adducts **6a**–**c** were obtained in >90% yield. Single crystals suited for an X-ray crystal structure analysis were obtained of the 1,4,5-trimethylimidazole/$B(C_6F_5)_3$ adduct **6a** from benzene at ambient temperature. Diffusion of pentane vapor into a toluene solution gave single crystals of the 1-methylbenzimidazole/$B(C_6F_5)_3$ addition compound **6c**.

† NMR spectroscopy.
‡ X-Ray crystal structure analyses.
§ Quantum chemical calculations.

DOI: 10.1039/b210030b

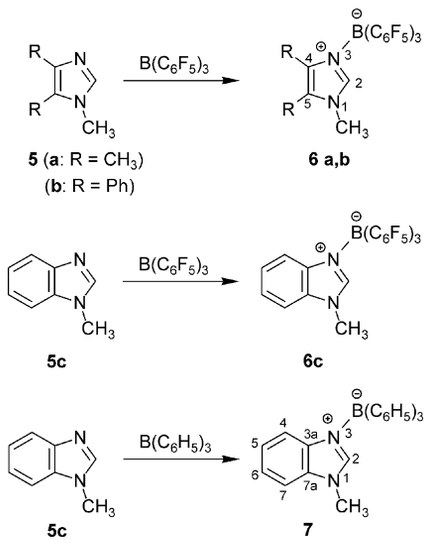

Scheme 2

The X-ray crystal structure analysis of compound **6a** shows that the bulky borane has become attached covalently to the trimethylimidazole nitrogen atom (N1–B: 1.588(2) Å, see Fig. 1). The imidazole framework shows the typical bond delocalization of a five-membered heteroaromatic system (for details see the legend of Fig. 1).[8]

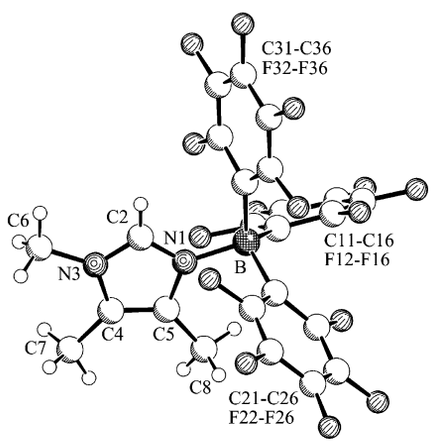

Fig. 1 A view of the molecular structure of compound **6a**. Selected bond lengths (Å) and angles (°): N1–B 1.588(2), N1–C2 1.324(2), N1–C5 1.397(2), C2–N3 1.322(2), N3–C4 1.386(3), C4–C5 1.355(3), N3–C6 1.459(2), C4–C7 1.482(3), C5–C8 1.492(3), B–C11 1.639(3), B–C21 1.652(2), B–C31 1.651(3); B–N1–C2 125.5(1), B–N1–C5 128.0(2), C2–N1–C5 106.5(2), N1–C2–N3 110.8(2), C2–N3–C4 108.4(2), N3–C4–C5 106.2(2), C4–C5–N1 108.2(2), N1–B–C11 112.1(1), N1–B–C21 103.6(1), N1–B–C31 108.3(1), C11–B–C21 113.9(1), C11–B–C31 104.3(1), C21–B–C31 114.8(1).

The most noteworthy structural feature about **6a** is the observed conformational arrangement of the four aryl moieties around the tetravalent boron center.[9] Tetraarylborates can adopt a chiral conformation where three of their planar substituents are found in an (idealized) C_3-symmetric three-bladed propeller arrangement. The remaining aryl ring cannot participate in this arrangement and serves as a pivot. Complex **6a** in particular shows a conformational topology that is related to such an arrangement, only that the (distorted) three-bladed propeller orientation is made up by two of the C_6F_5 substituents *and* the imidazole heteroaryl ring system.

Thus, the third C_6F_5 group (C11–C16) is taking up the pivot function. It can be seen from the projection in Fig. 1, that the N1–B vector is oriented almost coplanar with the C11–C16 plane (dihedral angles N1–B–C11–C12: −175.9(1)°, C2–N1–B–C11: −119.9(2)°). We will term this substituent at boron the $(C_6F_5)_{piv}$ group. The other two C_6F_5 substituents are part of the propeller geometry, but their position and orientation are quite different from one another. The C31–C36 ring system (see Fig. 1) has its connecting B–C31 vector oriented almost in the imidazole plane (dihedral angle C2–N1–B–C31: −5.5(2)°), whereas the adjacent C21–C26 C_6F_5 group is oriented *gauche* to this plane (along to the connecting N1–B vector). We will denote the former as the $(C_6F_5)_{in\ plane}$ group and the latter the $(C_6F_5)_{gauche}$ substituent. The corresponding dihedral angle C2–N1–B–C21 amounts to 116.9(2)°. For illustration of this specific conformational geometry a different view of the structure of compound **6a** is depicted in Fig. 2. The distorted three-bladed propeller geometry that contains the imidazole ring, the C31–C36 $(C_6F_5)_{in\ plane}$ and the C21–C26 $(C_6F_5)_{gauche}$ substituents at the central boron atom is characterized by dihedral angles of −62.0(2)° (N1–B–C31–C36), 115.7(2)° (N1–B–C21–C26) and 116.9(2)° (C21–B–N1–C2).

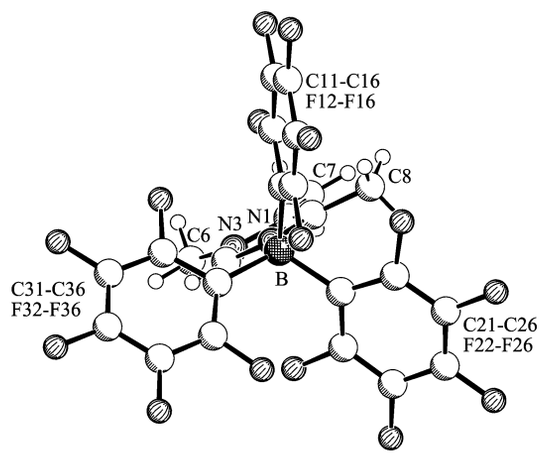

Fig. 2 A projection of the structure of compound **6a** along the B–N1 vector showing the distorted three-bladed propeller arrangement made up by the imidazole, the $(C_6F_5)_{in\ plane}$ (C31–C36) and the $(C_6F_5)_{gauche}$ (C21–C26) groups.

The 1-methylbenzimidazole/$B(C_6F_5)_3$ adduct shows an analogous structure. Attachment of the Lewis acid to the ring nitrogen has again only resulted in a marginal alteration of the typical imidazole structural parameters. The most remarkable solid state structural feature of **6c** is the observed conformational arrangement of the [(aryl)$_3$/heteroaryl)] orientation around boron (Fig. 3). It is almost identical to that observed of

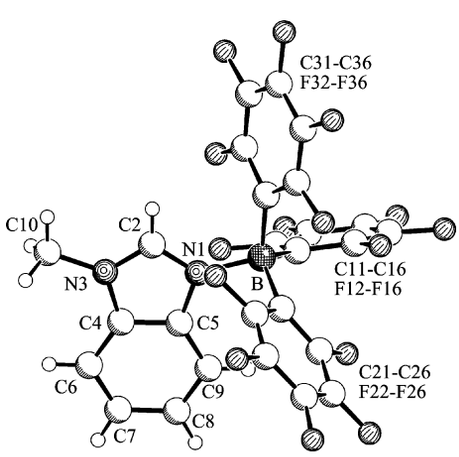

Fig. 3 Projection of the molecular structure of compound **6c**. Selected bond lengths (Å) and angles (°): N1–B 1.600(3), N1–C2 1.324(3), N1–C5 1.402(3), C2–N3 1.337(3), N3–C4 1.384(3), C4–C5 1.395(3), N3–C10 1.464(3), C4–C6 1.395(3), C5–C9 1.393(3), B–C11 1.641(3), B–C21 1.647(3), B–C31 1.651(3); B–N1–C2 128.2(2), B–N1–C5 125.2(2), C2–N1–C5 106.4(2), N1–C2–N3 112.0(2), C2–N3–C4 107.7(2), N3–C4–C5 106.3(2), C4–C5–N1 107.6(2), N1–B–C11 110.5(2), N1–B–C21 102.5(2), N1–B–C31 110.9(2), C11–B–C21 116.1(2), C11–B–C31 104.2(2), C21–B–C31 112.9(2).

compound **6a**. In **6c** again a distorted three-bladed propeller geometry is made up by the heteroaryl ring and two of the C_6F_5 planes. Again, the C31–C36 ring is placed with its B–C31 vector *syn*-oriented with the (benz)imidazole N1–C2(H) vector (dihedral angle C31–B–N1–C2 −4.8(3)°) and this $(C_6F_5)_{\text{in plane}}$ ring is rotated by 131.3(2)° (*i.e.* N1–B–C31–C32) from the N1–B vector. The C21–C26 group makes up the $(C_6F_5)_{gauche}$ part (C2–N1–B–C21 115.9(2)°, N1–B–C21–C22 −63.2(2)°) that complements the chiral substructure of **6c**. The remaining C11–C16 C_6F_5 substituent serves as the pivot in the aryl$_4$B-type structure of **6c**.

The B(aryl)$_3$(heteroaryl) systems all seem to adopt this characteristic conformational type in the crystal, regardless of the presence of C_6F_5 groups. We have to deduce this from the typical structure of the 1-methylbenzimidazole/B$(C_6H_5)_3$ adduct **7** (see Fig. 4). Here, a C_6H_5 group (C11–C16) serves as the pivot, whereas the C31–C36 C_6H_5 substituent is oriented close to "in plane" (C2–N1–B–C31 −20.4(2)°, N1–B–C31–C32 −91.7(2)°) and the remaining C21–C26 ring is $(C_6H_5)_{gauche}$.

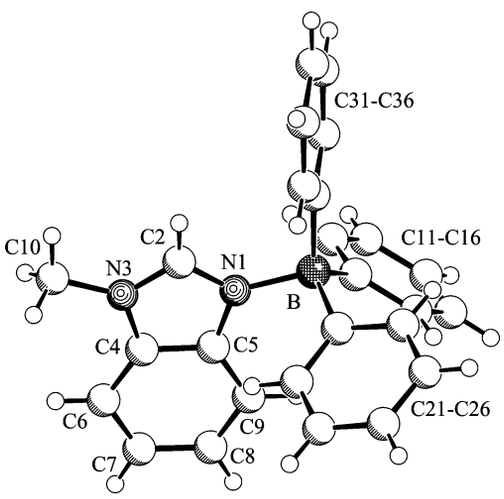

Fig. 4 A view of the molecular structure of the methylbenzimidazole/B$(C_6H_5)_3$ adduct **7**. Selected bond lengths (Å) and angles (°): N1–B 1.623(2), N1–C2 1.324(2), N1–C5 1.403(2), C2–N3 1.334(2), N3–C4 1.383(2), C4–C5 1.396(2), N3–C10 1.456(2), C4–C6 1.388(2), C5–C9 1.391(2), B–C11 1.627(2), B–C21 1.630(2), B–C31 1.637(2); B–N1–C2 126.6(1), B–N1–C5 126.7(1), C2–N1–C5 106.0(1), N1–C2–N3 112.4(2), C2–N3–C4 107.7(1), N3–C4–C5 106.2(1), C4–C5–N1 107.7(1), N1–B–C11 105.1(1), N1–B–C21 106.3(1), N1–B–C31 108.0(1), C11–B–C21 114.1(1), C11–B–C31 112.3(1), C21–B–C31 110.6(1).

Dynamic behavior in solution

The ^{1}H NMR spectrum of the benzimidazole/B$(C_6F_5)_3$ adduct (**6c**) shows the signal of the "isolated" 2-H proton at δ 7.61. The corresponding ^{13}C NMR resonance is observed at δ 141.9. In addition we find the aromatic 4-H (δ 7.64) 5-/6-H (δ 6.88) and 7-H (δ 6.47) signals and the N–CH_3 ^{1}H NMR resonance (δ 2.18) at the expected positions. The ^{19}F NMR spectra, though, reveal a remarkable conformational behavior of the addition compound **6c**. The fluorine NMR spectra of this compound were examined in the temperature range between 243 and 373 K at 563.6 MHz using a toluene-d_8 solution. As depicted in Fig. 5 the fluorine NMR signals of compound **6c** are nicely separated into three sets of resonances corresponding to the *ortho*-, *para*- and *meta*-F substituents of the three C_6F_5 groups at the central boron atom.

Moreover, in the low-temperature regime (243–253 K) 15 different fluorine NMR resonances are observed (see Fig. 5), which indicates that a chiral tetraarylborate conformation has become frozen on the ^{19}F NMR time scale. We must assume that under these conditions rotation around all three C(aryl)–B bonds is frozen out *and* the rotation around the benzimidazole N–B vector as well. This makes all three C_6F_5 groups

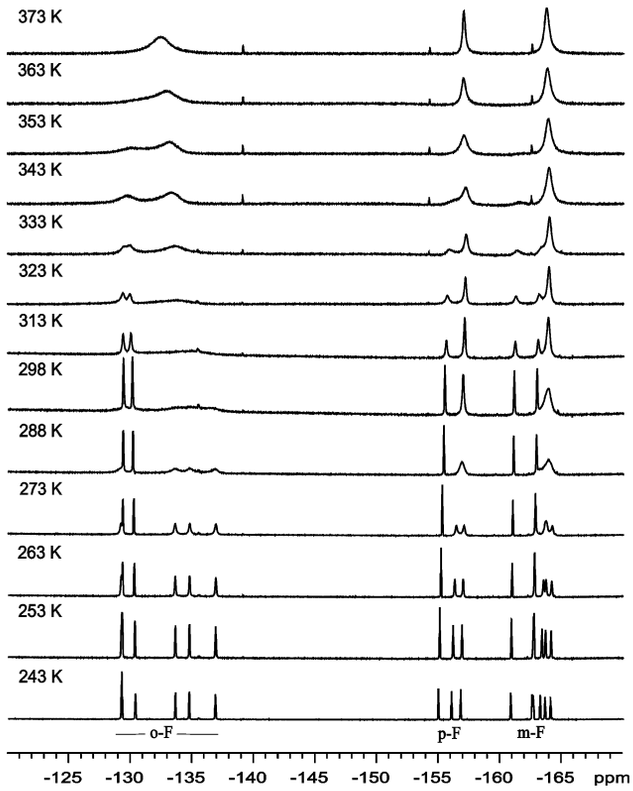

Fig. 5 Temperature-dependent dynamic ^{19}F NMR spectra of compound **6c** in toluene-d_8 solution.

diastereotopic *and* it makes the *ortho*- and *meta*-fluorines on each of the C_6F_5 substituents diastereotopic as well. A conformation as found of the compounds **6** and **7** in the solid state would account for the observation of these two sets of topological diastereotopisms under static conditions in solution. Thus, we may assume that the compound **6c** adopts similar chiral conformational structures in solution and in the solid state and that this may probably be characterized by the specific geometric features as they are depicted in Fig. 3 (see above).

Upon raising the temperature, four out of the six *ortho*-fluorine signals broaden and eventually coalesce to a single averaged signal of then four-fold intensity. Likewise two of the *para*-fluorine NMR signals coalesce and four of the *meta*-^{19}F resonances coalesce to a single averaged resonance. Upon inspection of the series of ^{19}F NMR spectra, we thus notice that at some intermediate temperature in the investigated temperature range we are principally observing a set of *ortho*, *meta* and *para* resonances of a relative intensity of two originating from a pair of conformationally equilibrating C_6F_5 groups [^{19}F NMR signals at *ca.* δ −133 (*ortho*), δ −157 (*para*) and δ −164 (*meta*), see *e.g.* the spectrum at 313 K in Fig. 5] in addition to a differentiated set of two *ortho* (δ −129, −130), one *para* (δ −155) and two *meta* (δ −161, −163) ^{19}F NMR resonances of relative intensity one. These latter five signals correspond to the third C_6F_5-group of compound **6c** at boron, which is neither conformationally equilibrating with its pair of neighboring C_6F_5 groups nor shows rapid rotation around the B–C bond at this temperature on the ^{19}F NMR time scale. Thus we have the curious situation that in compound **6c** in this specific temperature range two of the C_6F_5 groups are exhibiting rapid rotation around the B–C bonds in conjunction with rapid rotation around the N–B vector, which leads to pairwise equilibration of the *ortho*- and *meta*-fluorines in each ring *and* loss of the characteristic diastereotopic differentiation between these two individual C_6F_5 rings, while the third C_6F_5 ring remains conformationally "locked" in its rotated position along its connecting B–C vector.

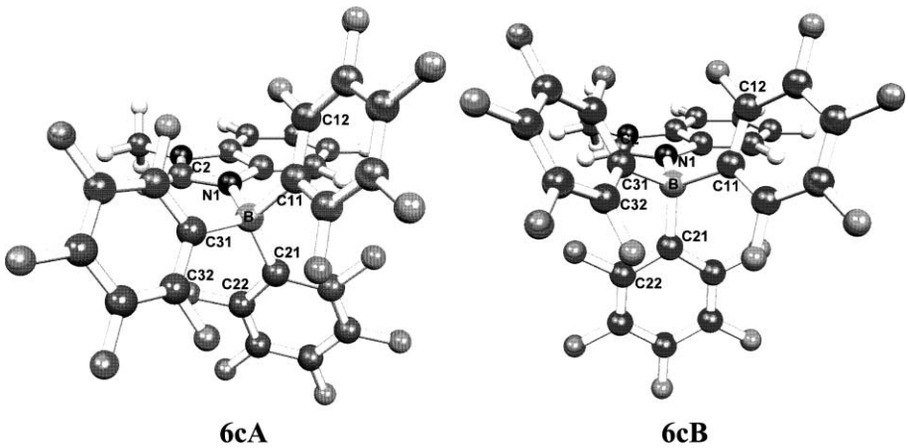

6cA **6cB**

Fig. 6 DFT-calculated structures of the two conformers of 1-methylbenzimidazole/$B(C_6F_5)_3$ adduct **6cA** and **6cB**. Structural parameters are given in Table 2.

Table 1 Gibbs activation energies ($\Delta G^{\ddagger}$ in kcal mol^{-1}) of the two conformational equilibration processes observed in the compounds **6** by dynamic ^{19}F NMR spectroscopy[a]

Compound	$\Delta G^{\ddagger}_a$ (T_c/K)	$\Delta G^{\ddagger}_b$ (T_c/K)
6a	10.2 (233)	17.0 (373)
6b	13.8 (303)	17.4 (383)
6c	13.0 (273)	15.9 (343)

[a] $\Delta G^{\ddagger} \pm 0.3$ kcal mol^{-1}; for details see the text.

Raising the temperature further eventually results in an overcoming of the activation barrier of this last remaining restricted B–C_6F_5 rotation which leads to complete conformational equilibration and thus a joining of the remaining five separate ^{19}F NMR signals into the general coalescence. At the highest investigated temperature (373 K) we thus have monitored a single set of three averaged *ortho*, *para* and *meta* C_6F_5 signals in a 2 : 1 : 2 intensity ratio (see Fig. 5).

Line shape analysis of the *para* ^{19}F NMR resonances[10] gave us the activation energies of the two spectroscopically differentiated dynamic processes that were observed by the dynamic ^{19}F NMR spectra of **6c**. The lower energy barrier of the two, which corresponds to a B–N and B–C rotational process equilibrating two of the C_6F_5 groups, has a Gibbs activation energy of $\Delta G^{\ddagger}_a$ (273 K) = 13.0 ± 0.3 kcal mol^{-1}. Overcoming the B–C rotational barrier of the remaining B–C_6F_5 unit is characterized by a slightly higher activation energy of $\Delta G^{\ddagger}_b$ (343 K) = 15.9 ± 0.3 kcal mol^{-1}.

The compounds **6a** and **6b** show the same type of conformational behavior. Each of these compounds exhibits 15 equal intensity ^{19}F NMR signals at low temperature. Raising the monitoring temperature in each case results in a coalescence of the signals of two C_6F_5 groups combined with pairwise *ortho*- and *meta*-F coalescence (process a), followed by a separated coalescence of the remaining C_6F_5 group at distinctly higher temperature (process b). The Gibbs activation energies of these processes were also obtained from a line shape analysis of their respective sets of *para* ^{19}F NMR signals. The $\Delta G^{\ddagger}_a$ and $\Delta G^{\ddagger}_b$ values of the compounds **6a** and **6b** are in a similar order of magnitude as observed of the benzimidazole/$B(C_6F_5)_3$ adduct **6c** (see Table 1).

Theoretical studies

We have carried out a theoretical study using density functional theory (DFT) to achieve some mechanistic insight into the conformational processes that determine the observed unusual dynamic behavior of the methylimidazole/$B(C_6F_5)_3$ adducts **6** that we had monitored by ^{19}F NMR spectroscopy in solution. We have investigated **6a** and **6c** which behave very similarly, but limit our discussion to compound **6c**. A detailed conformational search (B3LYP/TZVP) produced two minima **6cA** and **6cB** which are separated by 3.5 kcal mol^{-1}, the former being more stable. Fig. 6 shows a view of the two calculated structures.

Table 2 Selected calculated bond lengths (Å), angles and dihedral angles (°) of conformers **6cA** and **6cB**

	6cA (Calc.)	**6c** (X-ray)	**6cB** (Calc.)
N1–B	1.621	1.600(3)	1.627
C2–N1	1.322	1.324(3)	1.324
C2–N1–B	126.3	128.2(2)	121.9
N1–B–C11	111.8	110.5(2)	112.4
N1–B–C21	101.3	102.5(2)	100.6
N1–B–C31	109.4	110.9(2)	110.2
Θ_1 (C2–N1–B–C31)	−12.1	−4.8(3)	−40.9
Θ_2 (C2–N1–B–C21)	109.2	115.9(2)	80.8
Θ_3 (C2–N1–B–C11)	−126.8	−119.8(2)	−154.9
Φ_1 (N1–B–C31–C32)	132.1	131.3(2)	160.2
Φ_2 (N1–B–C21–C22)	−63.5	−63.2(2)	−88.0
Φ_3 (N1–B–C11–C12)	13.3	6.9(2)	43.2

Obviously, **6cA** corresponds to the conformation found in the crystal. The agreement between the calculated and solid state structures is quite good. The largest discrepancies are found for the dihedral angle Θ_1 and Φ_3 (about 10°) which may be attributed to crystal packing effects. Conformer **6cB** shows almost local C_s symmetry of the $B(C_6F_5)_3$ moiety as can be concluded from Fig. 6. **6cB** can be reached from **6cA** by a 30° rotation around the B–N vector with a tiny barrier for the back rotation **6cB** ⟶ **6cA** of 0.2 kcal mol^{-1}. The calculated structure **6cA** did not reveal any exceptionally close contacts between fluorine atoms and the imidazole nucleus or its periphery that could account for any of the unusual dynamic behavior exhibited by this compound. We have therefore examined a variety of specific single N–B and B–C rotational processes to check whether any specific unfavorable interaction could be detected that would explain why one of the C_6F_5 rings would not give up so easily its "left/right" separation whereas the others did. No specific pathway could, however, be detected that would indicate a necessary raising in energy to account for the observed behavior.

Due to the enormous complexity of the total conformational surface of the compounds **6** we did not attempt to calculate the overall favored internal equilibration pathway that is generally followed in these unsymmetrical tetraarylborate type compounds, but it seems clear that a highly cooperative mechanism must be followed here that results in the observed unusual, very specific conformational features of these molecules.

To illustrate this, we have performed a molecular dynamics simulation of compound **6c** at the semiempirical MNDO[11]

Table 3 ^{19}F NMR spectra of the compounds **9a** and **9c**[a]

Compound	2′-F	3′-F	4′-F	5′-F	*o*-F[b]	*m*-F[b]	*p*-F[b]
9a	−132.6	−157.2	−151.2	−134.8	−132.8	−164.0	−157.5
9c	−131.7	−156.0	−148.2	−132.3	−132.7	−163.5	−157.2

[a] **9a** in benzene-d_6–THF-d_8 (10 : 1), **9c** in toluene-d_8–THF-d_8 (10 : 1) at 563.6 MHz, ambient temperature. [b] C_6F_5 groups.

level. After equilibration (50 ps), values for Θ_1, Φ_1, Φ_2 and Φ_3 were followed for additional 50 ps. The results shown in Fig. 7 clearly demonstrate the cooperative motion of the three aryl rings and the propeller as a whole. Although in our MD simulation no full rotation event has been observed, the moderate twisting motions of the rings (about 10–20° amplitude with a period of about 2 ps) occur fully correlated.

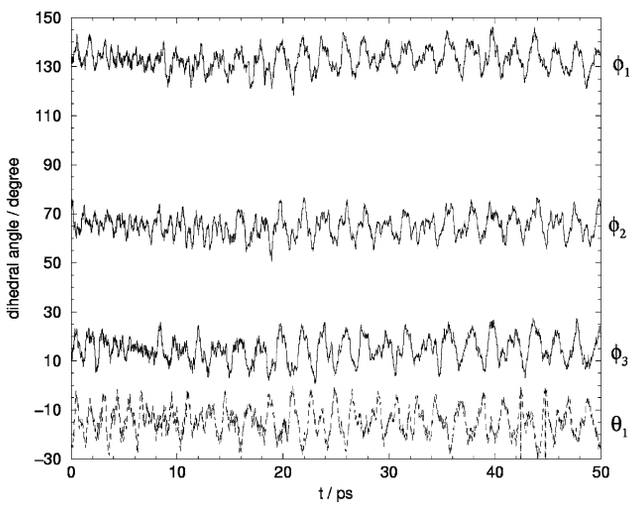

Fig. 7 Dihedral angles Θ_1 and Φ_1–Φ_3 along a 50 ps MNDO trajectory (*NVT* ensemble, T = 300 K) for compound **6c**. For clarity, the negative of Φ_2 is plotted.

In summary, our calculations did not reveal any evidence for a specific C–F interaction—be it in the ground state or at some point along potential rotational pathways—with other groups of the molecules that could account for the observed differentiation in the rotational behavior of one pair of C_6F_5 groups against the remaining single pentafluorophenyl substituent. It remained as a possible explanation that these observed characteristic conformational features of **6** are due to a general topochemical control. A natural candidate for the specific C_6F_5 group that needed a slightly higher energy to rotate around the B–C vector would then be the $(C_6F_5)_{pivot}$ (Φ_3) unit. Unfortunately, much longer MD runs in the nanosecond range to check this hypothesis are computationally not feasible at present. Before additional experimental evidence becomes available to us this seems to be a reasonable assumption to account for the remarkable observed dynamic behavior of these compounds.

Reactions with bases

The compounds **6a** and **6c** were each treated with methyllithium. In each case the imidazole 2-H proton is selectively abstracted. We assume that this reaction generates the corresponding "Arduengo carbene anions" (**8a**, **8c**). However, these compounds are unstable under the applied reaction conditions due to a rapid intramolecular nucleophilic aromatic substitution reaction.[5,12] Attack of the C2 carbanion-type nucleophile takes place at the *ortho* C–F moiety of one of the C_6F_5 groups. Fluoride is eliminated and lithium fluoride precipitated. The resulting C–C coupled products (**9a**, **9c**, see Scheme 3) were isolated in high yield. They represent intramolecular imidazolium borates themselves, only that the N3–B interaction has

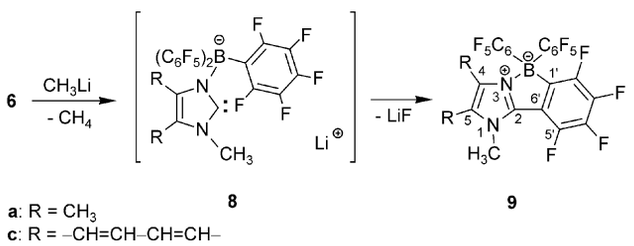

Scheme 3

closed a heterocyclic ring system due to the covalent attachment of the $(aryl)_3B$ moiety through the newly formed carbon–carbon bond between the adjacent imidazole C2 center and a boron bound aryl group.

The products **9** show very characteristic NMR spectra, including their ^{19}F NMR spectra (see Table 3). In addition, the tricyclic product **9c** was characterized by an X-ray crystal structure analysis (see Fig. 8).

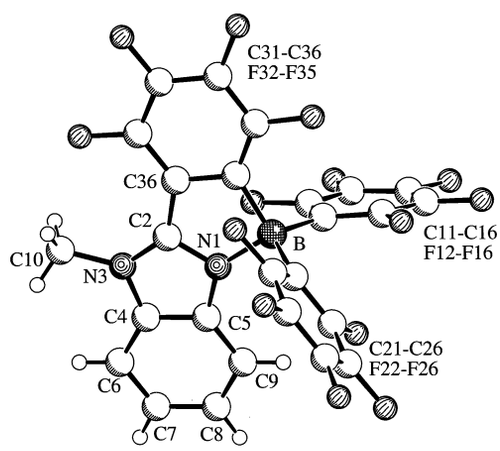

Fig. 8 Molecular structure of **9c**. Selected bond lengths (Å) and angles (°): N1–B 1.590(2), N1–C2 1.345(2), N1–C5 1.386(2), C2–N3 1.340(2), N3–C4 1.391(2), C4–C5 1.399(3), C2–C36 1.456(3), N3–C10 1.467(2), C4–C6 1.390(3), C5–C9 1.390(3), B–C11 1.629(3), B–C21 1.646(3), B–C31 1.625(3); B–N1–C2 112.9(1), B–N1–C5 139.3(2), C2–N1–C5 107.8(2), N1–C2–N3 110.8(2), C2–N3–C4 107.5(2), N3–C4–C5 107.1(2), C4–C5–N1 106.8(2), N1–C2–C36 111.9(2), N3–C2–C36 137.2(2), N1–B–C11 112.0(2), N1–B–C21 106.4(1), N1–B–C31 95.9(1), C11–B–C21 115.0(1), C11–B–C31 110.0(2), C21–B–C31 115.9(2).

Single crystals of **9c** that were suitable for X-ray crystal structure analysis were obtained by allowing pentane vapor diffuse into a toluene solution at 4 °C. The structural analysis shows the presence of a planar tricyclic ring system. The benzimidazole ring is connected with the C_6F_4 unit by means of the newly formed C2–C36 bond (see Fig. 8) and the B–N1 linkage. The latter amounts to 1.590(2) Å, which is marginally shorter than the N–B bond found in its precursor, the adduct **6c** (see above). In **9c** the remaining C_6F_5 groups at the boron center are also found in a rotated conformation, making the $B(C_6F_5)_2$ moiety a chiral subunit.

Experimental

Reactions with organometallic compounds were carried out in an inert atmosphere (argon) using Schlenk-type glassware or in a glovebox. Solvents, including deuterated solvents used for

NMR spectroscopy, were dried and distilled under argon prior to use. The following instruments were used for physical characterization of the compounds: Bruker AC 200 P NMR spectrometer (^{1}H: 200 MHz; ^{13}C: 50 MHz; ^{11}B: 64 MHz) at 300 K and Varian Unity plus (^{1}H: 600 MHz; ^{13}C: 150 MHz; ^{19}F: 564 MHz) NMR spectrometer at 298 K; a Nicolet 5 DXC FT–IR spectrometer; elemental analysis were carried out with a Foss-Heraeus CHN-rapid elemental analyzer or a Vario El III micro elemental analyzer; melting points were determined by differential scanning calorimetry (2010 DSC, Du Pont/STA Instruments). 1,4,5-Trimethylimidazole (**5a**),[13] 1-Methyl-4,5-diphenylimidazole (**5b**)[14] and tris(pentafluorophenyl)borane[6,15] were prepared according to literature procedures.

Preparations

1-Methylimidazole–borane derivatives 6a–c (general procedure). A suspension of the respective imidazole in 20 ml pentane was cooled to 0 °C and reacted with an equivalent amount of tris(pentafluorophenyl)borane. After stiring for 12 h at room temperature the solid was collected by filtration and the product was dried *in vacuo*.

1,4,5-Trimethylimidazole–tris(pentafluorophenyl)borane adduct (6a). Reaction of 110 mg (1.00 mmol) 1,4,5-trimethylimidazole (**5a**) with 512 mg (1.00 mmol) of tris(pentafluorophenyl)borane in pentane carried out as described above yielded 588 mg (95%) of the adduct **6a** as a white solid. mp: 232 °C. Anal. Calc. for $C_{24}H_{10}N_2BF_{15}$ (622.1): C, 46.33; H, 1.62; N, 4.50. Found: C, 46.19; H, 1.53; N, 3.17%. IR (KBr): $\tilde{\nu}$ 3176, 2935, 1647, 1563, 1524, 1458, 1373, 1283, 1097, 978, 870, 785 and 697 cm^{-1}. δ_H (benzene-d_6, 600 MHz): 7.12 (s, 1H, 2-H), 1.81 (s, 3H, NCH_3), 1.57 (s, 3H, 4-CH_3), 0.99 (s, 3H, 5-CH_3). δ_C (benzene-d_6, 150 MHz): 148.7 (dm, $^1J_{CF}$ = 244 Hz, *o*-Ph^F), 140.3 (dm, $^1J_{CF}$ = 249 Hz, *p*-Ph^F), 137.4 (dm, $^1J_{CF}$ = 249 Hz, *m*-Ph^F), 135.5 (CH, C-2), 131.4 (C, C-4), 125.8 (C, C-5), 119.4 (C, *ipso*-C), 31.1 (CH_3, NCH_3), 9.7 (CH_3, 4-Me), 6.9 (CH_3, 5-Me). δ_F (benzene-d_6, 564 MHz): −128.2 (m, 1F, *o*-Ph^F), −129.3 (br, 1F, *o*-Ph^F), −131.0 (m, 1F, *o*-Ph^F), −133.5, −134.3, −139.7 (each br, each 1F, each *o*-Ph^F), −155.7 (m, 1F, *p*-Ph^F), −156.9, −157.4 (each br, each 1F, each *p*-Ph^F), −161.4 (m, 1F, *m*-Ph^F), −163.3 (m, 1F, *m*-Ph^F), −163.6, −164.0, −164.5, −164.9 (each br, each 1F, each *m*-Ph^F). δ_B (benzene-d_6, 64 MHz): −8.7 ($\nu_{½}$ = 140 Hz).

X-Ray crystal structure analysis of **6a**: formula $C_{24}H_{10}BF_{15}N_2$, M = 622.15, colourless crystal 0.35 × 0.25 × 0.20 mm, a = 9.791(1), b = 19.826(1), c = 12.529(1) Å, β = 102.24(1)°, V = 2376.8(3) Å^3, D_c = 1.739 g cm^{-3}, μ = 1.85 cm^{-1}, empirical absorption correction *via* SORTAV (0.938 ≤ T ≤ 0.964), Z = 4, monoclinic, space group $P2_1/n$ (no. 14), λ = 0.71073 Å, T = 198 K, ω and φ scans, 22809 reflections collected (±h, ±k, ±l), [(sinθ)/λ] = 0.67 Å^{-1}, 5800 independent (R_{int} = 0.052) and 3695 observed reflections [$I \geq 2\sigma(I)$], 382 refined parameters, R = 0.043, $wR2$ = 0.093, max. residual electron density 0.25 (−0.28) e Å^{-3}, hydrogens calculated and refined as riding atoms.

1-Methyl-4,5-diphenylimidazole–tris(pentafluorophenyl)-borane adduct (6b). Treatment of 133 mg (568 μmol) 1-methyl-4,5-diphenylimidazole (**5b**) with 291 mg (568 μmol) tris(pentafluorophenyl)borane in pentane according to the general procedure yielded 399 mg (94%) of product **6b**. mp: 242 °C. Anal. Calc. for $C_{34}H_{14}N_2BF_{15}$ (746.29): C, 54.72; H, 1.89; N, 3.75. Found: C, 54.60; H, 1.68; N, 2.38%. IR (KBr): $\tilde{\nu}$ 3165, 1647, 1549, 1475, 1460, 1447, 1374, 1283, 1142, 1099, 983, 918, 807, 766 and 697 cm^{-1}. δ_H (benzene-d_6, 600 MHz): 7.55 (s, 1H, 2-H), 6.77 (m, 1H, *p*-Ph), 6.74 (m, 2H, *m*-Ph), 6.70 (br, 2H, *o*-Ph), 6.68 (m, 1H, *p*-Ph), 6.58 (m, 2H, *m*-Ph), 6.53 (m, 2H, *o*-Ph), 2.25 (s, 3H, NCH_3). δ_C (benzene-d_6, 150 MHz): 148.9 (dm, $^1J_{CF}$ = 239 Hz, *o*-Ph^F), 140.4 (dm, $^1J_{CF}$ = 252 Hz, *p*-Ph^F), 137.4 (dm, $^1J_{CF}$ = 245 Hz, *m*-Ph^F), 137.4 (C, C-4), 137.3 (CH, C-2), 133.5 (C, C-5), 130.6 (CH, *o*-Ph), 130.5 (CH, *o*-Ph), 129.3 (C, *ipso*-C), 129.3 (CH, *p*-Ph), 128.8 (CH, *p*-Ph), 128.4 (CH, *m*-Ph), 128.2 (CH, *m*-Ph), 126.0 (C, *ipso*-C), 120.1 (C, *ipso*-C), 32.7 (CH_3, NCH_3). δ_F (benzene-d_6, 564 MHz): −127.7 (m, 1F, *o*-Ph^F), −130.5 (m, 1F, *o*-Ph^F), −133.4 (br, 4F, *o*-Ph^F), −155.3 (m, 1F, *p*-Ph^F), −158.0 (m, 2F, *p*-Ph^F), −160.4 (m, 1F, *m*-Ph^F), −161.1 (m, 1F, *m*-Ph^F), −165.1 (br, 4F, *m*-Ph^F). δ_B (benzene-d_6, 64 MHz): −7.7 ($\nu_{½}$ = 240 Hz).

1-Methylbenzimidazole–tris(pentafluorophenyl)borane adduct (6c). Reaction of 437 mg (3.31 mmol) 1-methylbenzimidazole (**5c**) with 1.69 g (3.31 mmol) tris(pentafluorophenyl)borane in pentane carried out as described above yielded 1.92 g (90%) of the adduct **6c** as a white solid. mp: 231 °C. Anal. Calc. for $C_{26}H_8N_2BF_{15}$ (644.1): C, 48.48; H, 1.25; N, 4.35. Found: C, 48.04; H, 1.33; N, 4.16%. IR (KBr): $\tilde{\nu}$ 3000, 1649, 1557, 1517, 1424, 1392, 1284, 1100, 984, 864 and 748 cm^{-1}. δ_H (benzene-d_6, 600 MHz): 7.64 (d, $^3J_{HH}$ = 7.6 Hz, 1H, 4-H), 7.61 (s, 1H, 2-H), 6.88 (m, 2H, 5-H and 6-H), 6.47 (d, $^3J_{HH}$ = 7.3 Hz, 1H, 7-H), 2.18 (s, 3H, NCH_3). δ_C (benzene-d_6, 150 MHz): 148.8 (dm, $^1J_{CF}$ = 243 Hz, *o*-Ph^F), 141.9 (CH, C-2), 140.4 (dm, $^1J_{CF}$ = 248 Hz, *p*-Ph^F), 137.5 (dm, $^1J_{CF}$ = 253 Hz, *m*-Ph^F), 135.7 (C, C-7a), 132.5 (C, C-3a), 126.1 (CH, C-6), 125.7 (CH, C-5), 118.9 (C, *ipso*-C), 116.3 (CH, C-4), 111.6 (CH, C-7), 30.9 (CH_3, NCH_3). δ_F (benzene-d_6, 564 MHz): −129.5 (m, 1F, *o*-Ph^F), −130.5 (m, 1F, *o*-Ph^F), −134.7 (br, 4F, *o*-Ph^F), −155.7 (m, 1F, *p*-Ph^F), −157.2 (br, 2F, *p*-Ph^F), −161.5 (m, 1F, *m*-Ph^F), −163.1 (m, 1F, *m*-Ph^F), −164.1, (br, 4F, *m*-Ph^F). δ_B (benzene-d_6, 64 MHz): −7.9 ($\nu_{½}$ = 250 Hz).

X-Ray crystal structure analysis of **6c**: formula $C_{26}H_8BF_{15}N_2$, M = 644.15, colourless crystal 0.60 × 0.50 × 0.20 mm, a = 9.949(1), b = 15.245(1), c = 16.698(1) Å, β = 100.61(1)°, V = 2489.3(3) Å^3, D_c = 1.719 g cm^{-3}, μ = 1.80 cm^{-1}, empirical absorption correction *via* SORTAV (0.900 ≤ T ≤ 0.965), Z = 4, monoclinic, space group $P2_1/n$ (no. 14), λ = 0.71073 Å, T = 198 K, ω and φ scans, 15549 reflections collected (±h, ±k, ±l), [(sinθ)/λ] = 0.66 Å^{-1}, 5909 independent (R_{int} = 0.053) and 3742 observed reflections [$I \geq 2\sigma(I)$], 398 refined parameters, R = 0.050, $wR2$ = 0.113, max. residual electron density 0.31 (−0.24) e Å^{-3}, hydrogens calculated and refined as riding atoms.

1-Methylbenzimidazole–triphenylborane adduct (7). Triphenylborane (1.00 g, 4.13 mmol) was added to a suspension of 1-methylbenzimidazole (**5c**) (546 mg, 4.13 mmol) in 20 ml pentane at 0 °C. The reaction mixture was allowed to warm to room temperature and was stirred for another 12 h. The precipitate was collected by filtration to yield a white solid 1.27 g (82%). mp: 208 °C. Anal. Calc. for $C_{26}H_{23}N_2B$ (374.3): C, 83.43; H, 6.19; N, 7.48. Found: C, 82.00; H, 6.26; N, 7.06%. IR (KBr): $\tilde{\nu}$ 3065, 2997, 1539, 1487, 1461, 1425, 1382, 1256, 1187, 1160, 1082, 976, 857 and 747 cm^{-1}. δ_H (benzene-d_6, 600 MHz): 7.69 (m, 6H, *o*-Ph), 7.62 (s, 1H, 2-H), 7.32 (m, 6H, *m*-Ph), 7.37 (d, $^3J_{HH}$ = 8.5 Hz, 1H, 4-H), 7.22 (m, 3H, *p*-Ph), 6.79 (m, 1H, 6-H), 6.63 (m, 1H, 5-H), 6.49 (d, $^3J_{HH}$ = 8.3 Hz, 1H, 7-H), 2.03 (s, 3H, NCH_3). δ_C (benzene-d_6, 150 MHz): 153.4 (C, *ipso*-C), 143.1 (CH, C-2), 137.1 (C, C-7a), 135.2 (CH, *o*-Ph), 133.4 (C, C-3a), 127.5 (CH, *m*-Ph), 125.4 (CH, *p*-Ph), 124.7 (CH, C-6), 124.3 (CH, C-5), 121.5 (CH, C-4), 110.2 (CH, C-7), 30.4 (CH_3, NCH_3). δ_B (benzene-d_6, 64 MHz): 0.1 ($\nu_{½}$ = 470 Hz).

X-Ray crystal structure analysis of **7**: formula $C_{26}H_{23}BN_2$, M = 374.27, light yellow crystal 0.25 × 0.25 × 0.10 mm, a = 20.155(2), b = 14.400(1), c = 17.119(2) Å, β = 123.12(1)°, V = 4161.2(7) Å^3, D_c = 1.195 g cm^{-3}, μ = 5.27 cm^{-1}, empirical absorption correction *via* ψ scan data (0.880 ≤ T ≤ 0.949), Z = 8, monoclinic, space group $C2/c$ (no. 15), λ = 1.54178 Å, T = 223 K, $\omega/2\theta$ scans, 8590 reflections collected (±h, ±k, ±l), [(sinθ)/λ] = 0.62 Å^{-1}, 4241 independent (R_{int} = 0.033) and 2791 observed reflections [$I \geq 2\sigma(I)$], 264 refined parameters, R = 0.041, $wR2$ = 0.110, max. residual electron density 0.22 (−0.17) e Å^{-3}, hydrogens calculated and refined as riding atoms.

Treatment of compound 6a with methyllithium, formation of the heterocycle 9a. To a mixture of 100 mg (159 μmol) 1,4,5-trimethylimidazole–tris(pentafluorophenyl)borane adduct (**6a**) and 3.50 mg (159 μmol) of methyllithium 2 ml of benzene–tetrahydrofuran (10 : 1) was added. The resulting reaction mixture was allowed to stir for 12 h, the solvent was removed *in vacuo* and benzene was added. A lithium fluoride precipitate was separated by filtration and removal of the solvent yielded a light brown solid (85 mg, 89%). mp: 70 °C. Anal. Calc. for $C_{24}H_9N_2BF_{14}$ (602.1): C, 47.87; H, 1.51; N, 4.65. Found: C, 47.66; H, 2.81; N, 4.76%. IR (KBr): $\tilde{\nu}$ 2965, 1645, 1556, 1518, 1464, 1421, 1378, 1285, 1263, 1096, 1022, 976, 871 and 762 cm^{-1}. δ_H (benzene-d_6–tetrahydrofuran-d_8 10 : 1, 600 MHz): 2.99 (d, J_{HF} = 2.4 Hz, 3H, NCH_3), 1.75 (s, 3H, 5-CH_3), 1.45 (s, 3H, 4-CH_3). δ_C (benzene-d_6–tetrahydrofuran-d_8 10 : 1, 150 MHz): 148.9 (dm, $^1J_{CF}$ = 245 Hz, *o*-Ph^F), 145.5 (C, C-2), 140.3 (dm, $^1J_{CF}$ = 251 Hz, *p*-Ph^F), 137.6 (dm, $^1J_{CF}$ = 250 Hz, *m*-Ph^F), 129.5 (C, C-5), 128.3 (C, C-4), 115.2 (C, *ipso*-C), 32.2 (CH_3, J_{CF} = 17.2 Hz, NCH_3), 8.8 (CH_3, 5-CH_3), 8.1 (CH_3, 4-CH_3). The carbon-atoms C-1′ to C-6′ were not detected. δ_F (benzene-d_6–tetrahydrofuran-d_8 10 : 1, 564 MHz): −132.6 (m, 1F, F-2′), −132.8 (m, 4F, *o*-Ph^F), −134.8 (m, 1F, F-5′), −151.2 (m, 1F, F-4′), −157.2 (m, 1F, F-3′), −157.5 (m, 2F, *p*-Ph^F), −164.0 (m, 4F, *m*-Ph^F). δ_B (benzene-d_6–tetrahydrofuran-d_8 10 : 1, 64 MHz): −8.0 ($\nu_{½}$ = 130 Hz).

Treatment of compound 6c with methyllithium, formation of the heterocycle 9c. Analogous to the preparation of compound **9a**, 176 mg (272 μmol) of the 1-methylbenzimidazole–tris-(pentafluorophenyl)borane adduct (**6c**) was reacted with 6.00 mg (272 μmol) of methyllithium in 2 ml benzene–tetrahydrofuran (10 : 1). Workup of the suspension yielded in a brown solid (160 mg, 94%). mp: 61 °C. Anal. Calc. for $C_{26}H_7N_2BF_{14}$ (624.1): C, 50.03; H, 1.13; N, 4.49. Found: C, 50.79; H, 3.98; N, 4.05%. IR (KBr): $\tilde{\nu}$ 2965, 1645, 1608, 1575, 1550, 1518, 1460, 1423, 1383, 1315, 1291, 1098, 975, 796 and 751 cm^{-1}. δ_H (benzene-d_6–tetrahydrofuran-d_8 10 : 1, 600 MHz): 7.61 (m, 1H, 4-H), 7.02 (m, 2H, 5-H and 6-H), 6.93 (m, 1H, 7-H), 3.36 (d, J_{HF} = 3.6 Hz, 3H, NCH_3). δ_C (benzene-d_6–tetrahydrofuran-d_8 10 : 1, 150 MHz): 152.7 (C, C-2), 148.9 (dm, $^1J_{CF}$ = 240 Hz, *o*-Ph^F), 140.5 (dm, $^1J_{CF}$ = 251 Hz, *p*-Ph^F), 137.7 (dm, $^1J_{CF}$ = 247 Hz, *m*-Ph^F), 137.2 (C, C-7a), 133.6 (C, C-3a), 126.8 (CH, C-6), 125.7 (CH, C-5), 115.4 (C, *ipso*-C), 114.6 (CH, C-4), 112.5 (CH, C-7), 32.2 (CH_3, J_{CF} = 16.7 Hz, NCH_3). The carbon-atoms C-1′ to C-6′ were not detected. δ_F (benzene-d_6–tetrahydrofuran-d_8 10 : 1, 564 MHz): −131.7 (m, 1F, F-2′), −132.3 (m, 1F, F-5′), −132.7 (m, 4F, *o*-Ph^F), −148.2 (m, 1F, F-4′), −156.0 (m, 1F, F-3′), −157.2 (m, 2F, *p*-Ph^F), −163.5 (m, 4F, *m*-Ph^F). δ_B (benzene-d_6–tetrahydrofuran-d_8 10 : 1, 64 MHz): −8.3 ($\nu_{½}$ = 180 Hz).

X-Ray crystal structure analysis of **9c**: formula $C_{26}H_7BF_{14}N_2$, M = 624.15, yellow crystal 0.25 × 0.20 × 0.10 mm, a = 11.259(3), b = 11.878(4), c = 17.461(4) Å, β = 99.00(2), V = 2306.4(11) $Å^3$, D_c = 1.797 g cm^{-3}, μ = 16.83 cm^{-1}, empirical absorption correction *via* ψ scan data (0.678 ≤ T ≤ 0.850), Z = 4, monoclinic, space group $P2_1/n$ (no. 14), λ = 1.54178 Å, T = 223 K, $\omega/2\theta$ scans, 9465 reflections collected (±h, ±k, −l), [(sinθ)/λ] = 0.62 $Å^{-1}$, 4708 independent (R_{int} = 0.036) and 3474 observed reflections [$I \geq 2\sigma(I)$], 389 refined parameters, R = 0.039, $wR2$ = 0.103, max. residual electron density 0.24 (−0.27) e $Å^{-3}$, hydrogens calculated and refined as riding atoms.

Data sets were collected with Enraf-Nonius CAD4 and Nonius KappaCCD diffractometers, the latter equipped with a rotating anode generator Nonius FR591. Programs used: data collection: EXPRESS (Nonius B.V., 1994) and COLLECT (Nonius B.V., 1998), data reduction: MolEN[16] and Denzo-SMN,[17] absorption correction for CCD data: SORTAV,[18] structure solution: SHELXS-97,[19] structure refinement: SHELXL-97,[20] graphics: SCHAKAL.[21]

CCDC reference numbers 181962–181965.

See http://www.rsc.org/suppdata/dt/b2/b210030b/ for crystallographic data in CIF or other electronic format.

DFT Calculations

Geometries were optimized with the Turbomole package of programs[22] without any symmetry restrictions. We have used the B3-LYP hybrid functional[23] together a Gaussian AO basis set of TZVP quality.[24] Comparative calculations using the B–P functional or the MNDO[11] semi empirical method gave similar results.

For the molecular dynamics simulation, a modified version of the Mopac 7.0 program[25] was used.

Acknowledgements

Financial support from the Fonds der Chemischen Industrie and the Deutsche Forschungsgemeinschaft is gratefully acknowledged.

References

1 A. J. Arduengo III, R. L. Harlow and M. Kline, *J. Am. Chem. Soc.*, 1991, **113**, 361; A. J. Arduengo III, H. V. R. Dias, R. L. Harlow and M. Kline, *J. Am. Chem. Soc.*, 1992, **114**, 5530; review: A. J. Arduengo III, *Acc. Chem. Res.*, 1999, **32**, 913.

2 D. Bourissou, O. Guerret, F. P. Gabbaï and G. Bertrand, *Chem. Rev.*, 2000, **100**, 39.

3 J. Huang, E. D. Stevens, S. P. Nolan and J. L. Petersen, *J. Am. Chem. Soc.*, 1999, **121**, 2674; M. Scholl, T. M. Trnka, J. P. Morgan and R. H. Grubbs, *Tetrahedron Lett.*, 1999, **40**, 2247; T. Weskamp, F. J. Kohl, W. Hieringer, D. Gleich and W. A. Hermann, *Angew. Chem.*, 1999, **111**, 2573; T. Weskamp, F. J. Kohl, W. Hieringer, D. Gleich and W. A. Hermann, *Angew. Chem., Int. Ed.*, 1999, **38**, 2416; M. Scholl, S. Ding, C. W. Lee and R. H. Grubbs, *Org. Lett.*, 1999, **1**, 953; L. Jafarpour, A. C. Hillier and S. P. Nolan, *Organometallics*, 2002, **21**, 442 and references therein. Reviews: W. A. Herrmann and C. Köcher, *Angew. Chem.*, 1997, **109**, 2256; W. A. Herrmann and C. Köcher, *Angew. Chem., Int. Ed. Engl.*, 1997, **36**, 2162; T. Weskamp, P. W. Böhm and W. A. Herrmann, *J. Organomet. Chem.*, 2000, **600**, 12.

4 A. Wacker, H. Pritzkow and W. Siebert, *Eur. J. Inorg. Chem.*, 1998, 843; A. Weiss, H. Pritzkow and W. Siebert, *Eur. J. Inorg. Chem.*, 2002, 1607; A. Wacker, C. G. Yan, G. Kaltenpoth, A. Ginsberg, A. M. Arif, R. D. Ernst, H. Pritzkow and W. Siebert, *J. Organomet. Chem.*, 2002, **641**, 195; see also: I. I. Padilla-Martinez, M. de Jeses Rosalez-Hoz, R. Contreras, S. Kerschl and B. Wrackmeyer, *Chem. Ber.*, 1994, **127**, 343; K. Okuda, R. Suzuki and M. Oda, *J. Chem. Soc., Chem. Commun.*, 1995, 2069; see for a comparison: H. Nöth and B. Wrackmeyer, *Chem. Ber.*, 1974, **107**, 3070; N. Kuhn, H. Kotowski, D. Bläser and R. Boese, *Z. Naturforsch., Teil B*, 1997, **52**, 351; I. I. Padilla-Martínez, A. Ariza-Castolo and R. Contreras, *Magn. Reson. Chem.*, 1993, **31**, 189.

5 D. Vagedes, G. Kehr, D. König, K. Wedeking, R. Fröhlich, G. Erker, C. Mück-Lichtenfeld and S. Grimme, *Eur. J. Inorg. Chem.*, 2002, 2015; see also: K. Fujita, S. Hikichi, M. Akita and Y. Moro-oka, *J. Chem. Soc., Dalton Trans.*, 2000, 1255; X. Zheng and G. E. Herberich, *Organometallics*, 2000, **19**, 3751; A. Wacker, H. Pritzkow and W. Siebert, *Eur. J. Inorg. Chem.*, 1999, 789; S. Solé, H. Gornitzka, O. Guerret and G. Bertrand, *J. Am. Chem. Soc.*, 1998, **120**, 9100; I. I. Padilla-Martínez, F. J. Martínez- Martínez, A. López-Sandoval, K. I. Girón-Castillo, M. A. Brito and R. Contreras, *Eur. J. Inorg. Chem.*, 1998, 1547; G. A. McGibbon, C. Heinemann, D. J. Lavorato and H. Schwartz, *Angew. Chem.*, 1997, **109**, 1572; G. A. McGibbon, C. Heinemann, D. J. Lavorato and H. Schwartz, *Angew. Chem., Int. Ed. Engl.*, 1997, **36**, 1478; G. Maier, J. Endres and H. P. Reisenauer, *Angew. Chem.*, 1997, **109**, 1788; G. Maier, J. Endres and H. P. Reisenauer, *Angew. Chem., Int. Ed. Engl.*, 1997, **36**, 1709; L. Weber, E. Dobbert, H.-G. Stammler, B. Neumann, R. Boese and D. Bläser, *Chem. Ber./Rec*, 1997, **130**, 705; W. P. Fehlhammer, H. Hoffmeister U. Eckert and C. Robl, *Z. Naturforsch., Teil B*, 1993, **48**, 1448.

6 A. G. Massey, A. J. Park and F. G. A. Stone, *Proc. Chem. Soc. London*, 1963, 212; A. G. Massey and A. J. Park, *J. Organomet. Chem.*, 1964, **2**, 245; A. G. Massey and A. J. Park, *Organometallic Syntheses*, ed. R. B. King and J. J. Eisch, Elsevier, New York, 1986, vol. 3, p. 461.

7 For other $B(C_6F_5)_3$/Lewis-base adduct chemistry, see: *e.g.* K. Ishihara, N. Hananki and H. Yamamoto, *Synlett*, 1993, 577; K. Ishihara, N. Hananki and H. Yamamoto, *Synlett*, 1994, 963; T. Nagata, T. Toshihiro, T. Yamada, K. Imagawa and T. Mukaiyama, *Bull. Chem. Soc. Jpn.*, 1994, **67**, 2614; L. Li and T. J. Marks, *Organometallics*, 1998, **17**, 3996; D. J. Parks, W. E. Piers, M. Parvez, R. Atencio and M. J. Zaworotko, *Organometallics*, 1998, **17**, 1369; L. H. Doerrer and M. L. H. Green, *J. Chem. Soc., Dalton Trans.*, 1999, 4325; C. Bergquist and G. Parkin, *J. Am. Chem. Soc.*, 1999, **121**, 6322; C. Bergquist, B. M. Bridgewater, C. J. Harlan, J. R. Norton, R. A. Friesner and G. Parkin, *J. Am. Chem. Soc.*, 2000, **122**, 10581; R. E. La Pointe, G. R. Roof, K. A. Abboud and J. Klosin, *J. Am. Chem. Soc.*, 2000, **122**, 9560; J. Zhou, S. J. Lancaster, D. A. Walker, S. Beck, M. Thornton-Pett and M. Bochmann, *J. Am. Chem. Soc.*, 2001, **123**, 223; B. Y. Lee, G. C. Bazan, J. Vela, J. A. Komon and X. Bu, *J. Am. Chem. Soc.*, 2001, **123**, 5352; D. Vagedes, G. Erker and R. Fröhlich, *J. Organomet. Chem.*, 2002, **641**, 148; D. Vagedes, G. Erker and R. Fröhlich, *J. Organomet. Chem.*, 2002, **651**, 157; J. M. Blackwell, W. E. Piers, M. Parvez and R. McDonald, *Organometallics*, 2002, **21**, 1400.
8 F. H. Allen, O. Kennard, D. G. Watson, L. Brammer, A. G. Orpen and R. Taylor, *J. Chem. Soc., Perkin Trans 2*, 1987, S 1.
9 See, for a comparison: E. L. Eliel and S. H. Wilen, *Stereochemistry of Organic Compounds*, Wiley, New York, 1994, ch. 14-6, pp. 1156–1160.
10 DNMR3: D. A. Kleier and G. Binsch, Indiana University 1970; D. A. Kleier and G. Binsch, *J. Magn. Reson.*, 1970, **3**, 146; XSINM: K. Marat, University of Manitoba 1997; M. L. H. Green, L.-L. Wong and A. Seela, *Organometallics*, 1992, **11**, 2660 and references therein.
11 M. J. S. Dewar and W. Thiel, *J. Am. Chem. Soc.*, 1977, **99**, 4899.
12 For a related reaction of a $B(C_6F_5)_3$/ylide adduct, see: S. Döring, G. Erker, R. Fröhlich, O. Meyer and K. Bergander, *Organometallics*, 1998, **17**, 2183.
13 E. Schaumann, in *Methoden der Organischen Chemie (Houben-Weyl)*, 1994, E8c 6.
14 W. L. Collibee and J.-P. Anselme, *Tetrahedron Lett.*, 1985, **26**, 1595.
15 J. L. W. Pohlmann and F. E. Brinckmann, *Z. Naturforsch., Teil B*, 1965, **20**, 5; J. Lambert, S. Zhang and S. M. Ciro, *Organometallics*, 1994, **13**, 2430.
16 MolEN: K. Fair, Enraf-Nonius B.V., Delft, 1990.
17 Denzo-SMN: Z. Otwinowski and W. Minor, *Methods Enzymol.*, 1997, **276**, 307–326.
18 SORTAV: R. H. Blessing, *Acta Crystallogr., Sect. A*, 1995, **51**, 33–37; R. H. Blessing, *J. Appl. Crystallogr.*, 1997, **30**, 421–426.
19 SHELXS-97: G. M. Sheldrick, *Acta Crystallogr., Sect. A*, 1990, **46**, 467–473.
20 SHELXL-97: G. M. Sheldrick, Universität Göttingen, 1997.
21 SCHAKAL: E. Keller, Universität Freiburg, 1997.
22 Turbomole 5.5: Universität Karlsruhe, 1997.
23 A. D. Becke, *J. Chem. Phys.*, 1993, **98**, 5648; P. J. Stephens, F. J. Devlin, C. F. Chabalowski and M. J. Frisch, *J. Phys. Chem.*, 1994, **98**, 11623.
24 A. Schäfer, C. Huber and R. Ahlrichs, *J. Chem. Phys.*, 1994, **100**, 5829.
25 J. J. P. Stewart, MOPAC: A General Molecular Orbital Package, *Quant. Chem. Prog. Exch.*, 1990, **10**, 86.